Citation: Molecular Therapy — Methods & Clinical Development (2016) **3,** 16035; doi:10.1038/mtm.2016.35
Official journal of the American Society of Gene & Cell Therapy
www.nature.com/mtm

ARTICLE

Rapid, scalable, and low-cost purification of recombinant adeno-associated virus produced by baculovirus expression vector system

Pierre-Olivier Buclez[1], Gabriella Dias Florencio[2], Karima Relizani[1], Cyriaque Beley[1], Luis Garcia[2] and Rachid Benchaouir[1]

Recombinant adeno-associated viruses (rAAV) are largely used for gene transfer in research, preclinical developments, and clinical trials. Their broad *in vivo* biodistribution and long-term efficacy in postmitotic tissues make them good candidates for numerous gene transfer applications. Upstream processes able to produce large amounts of rAAV were developed, particularly those using baculovirus expression vector system. In parallel, downstream processes present a large panel of purification methods, often including multiple and time consuming steps. Here, we show that simple tangential flow filtration, coupled with an optimized iodixanol-based isopycnic density gradient, is sufficient to purify several liters of crude lysate produced by baculovirus expression vector system in only one working day, leading to high titers and good purity of rAAV products. Moreover, we show that the viral vectors retain their *in vitro* and *in vivo* functionalities. Our results demonstrate that simple, rapid, and relatively low-cost methods can easily be implemented for obtaining a high-quality grade of gene therapy products based on rAAV technology.

Molecular Therapy — Methods & Clinical Development (2016) **3**, 16035; doi:10.1038/mtm.2016.35; published online 11 May 2016

INTRODUCTION

Recombinant adeno-associated viruses (rAAV) are powerful tools for gene transfer and are currently used in research, preclinical, and clinical developments. These vectors display significant advantages: they are well tolerated after *in vivo* delivery, allow long-lasting gene expression, and numerous serotypes with specific tropisms are also available.[1] The first marketing approval for rAAV gene therapy has recently been delivered for the treatment of familial lipoprotein lipase deficiency.[2,3] It is likely that similar therapies will soon be approved for other pathologies,[4] calling for vector production improvements. Scale-up processes are rapidly evolving even though needs are different according to the type of disease to treat. Indeed, the rescue of Leber's Congenital Amaurosis defect by rAAV vectors only requires the injection of less than one milliliter of product underneath the retina,[5–7] while treatment of Duchenne muscular dystrophy is more challenging and would obviously solicit much higher volumes of viral vectors to target the whole body musculature.[8] Different upstream processes exist to meet the quantitative requirements in viral vectors. Small-scale productions can be performed through the classical tri-transfection method in adherent human embryonic kidney 293 (HEK293) cell line.[9–11] For large-scale productions, methods using baculovirus expression vector system were successfully implemented to produce rAAVs by insect cell lines grown in suspension.[12,13] Alternative methods using specific HEK293 cells strains able to grow in suspension were also described.[14] Other studies have shown the potential for producing rAAV vectors by stable cell lines[15] or the use of Herpes simplex virus for manufacturing productions.[16] On another hand, downstream processes propose a large panel of methods. Among them, chromatographic approaches are generally preferred when the levels of production become compatible with industrial scales. The most efficient ones use either ion exchange[17–19] or affinity methods.[20–22] Nevertheless, these techniques have the drawback of being relatively serotype-specific and require the implementation of other purification techniques, thus accentuating yield losses. Besides that, the costs of specific resins used to pack columns are quite expensive and detrimental during the launch of a clinical project. Finally, despite some described analysis methods,[23] these approaches currently remain ineffective for the separation of empty particles from full ones. Thus, implementation of alternative purification approaches for large-scale productions should be proposed to circumvent the qualitative, quantitative, and financial constraints mentioned above. One option is to simply use the physical properties of the viral particles to provide processes based on their density or sedimentation rate. Indeed, ultracentrifugation systems based on density gradients are successfully used for rAAV purification at research scale; iodixanol-based gradients appeared more suited for AAV vectors than the conventional cesium chloride (CsCl)-based gradients.[24,25] In this context, we recently showed that a simplified AAV purification process from HEK293T producer cells, using an isopycnic iodixanol gradient, led to high vector recovery and an unexpected improvement of *in vitro* and *in vivo*

[1]SQY Therapeutics, UFR des Sciences de la Santé, Montigny-le-Bretonneux, France; [2]Université de Versailles Saint-Quentin en Yvelines, U1179 INSERM/UVSQ, UFR des Sciences de la Santé, Montigny-le-Bretonneux, France. Correspondence: R Benchaouir (rachid.benchaouir@uvsq.fr)
Received 4 January 2016; accepted 1 April 2016

functionalities compared to classical described protocols.[26] The ultracentrifugation process is generally considered too difficult or even impossible to be implemented in the handling of large-scale productions. The relatively low volume of supernatant that can be treated by a single run of ultracentrifuge explains in large part the reluctance of users to choose this technology when processing large volumes. Nevertheless, equipments designed to highly concentrate big volumes of biological solutions are now available, making it possible to consider ultracentrifugation as a feasible method for the final purification step. Indeed, this approach has been successfully applied to purify rAAV from several liters of crude lysates, although the process extended over 1 week.[27]

Here, we show that implementation of an optimized isopycnic gradient construction led the process to be advantageously used for treating large initial volumes of vector as well as reducing the entire purification step to one working day. Compared to purification based on conventional iodixanol gradients,[25] our method equally preserved high final product quality and the rAAV particles remained functional as shown by *in vitro* and *in vivo* transduction assays.

RESULTS

Optimized isopycnic gradient method for efficient rAAV purification

The rAAV upstream process was performed by using the baculovirus expression vector system (Supplementary Figure S1). We used different recombinant baculoviruses, one harboring the codon-optimized *rep2* and *cap9* genes under potent baculovirus promoters[12,28] and the others harboring either the green fluorescent protein (GFP) or the mouse secreted alkaline phosphatase (mSEAP) reporter genes under a cytomegalovirus (CMV) promoter (Supplementary Figures S1 and S4). After generating the baculovirus-infected insect cells (BIIC),[29,30] rAAV productions were initiated by cocultivation of two BIICs, including BIIC-Rep2$_{opt}$/Cap9$_{opt}$ with either BIIC-GFP or BIIC-mSEAP, with native Sf9 insect cells in a ratio of 1 to 10^4 v/v respectively. Of note, all cell cultures were performed in serum-free medium. Under these conditions, the upstream process was stopped 72 hours later, after which the downstream process was initiated. Figure 1a is a schematic representation of the downstream process. The latter is described in further detail in Supplementary Table S1. The first clarification step started with the addition of 0.5% Triton X-100 detergent in the culture to induce efficient cell lysis without altering the viral particles as we previously described.[26] After microfiltration, the clarified crude lysates with a volume greater than 100 ml were concentrated by tangential flow filtration. A 10 to 30× concentration factor was used to prepare the vector solution for the next purification step. Finally, the research-scale (from 400 ml to 2 l) and pilot-scale (from 5l) productions were concentrated to 60 and 240 ml respectively. By adapting the hollow fiber filtration surfaces to volumes to be processed, the duration of the concentration process only differed from 1 to 2 hours depending on the initial volume of production (Supplementary Table S1).

The most significant downstream process improvement was achieved with the implementation of a new iodixanol isopycnic density gradient. A more conventional purification method, derived from the original work of Zolotukhin *et al.*,[25] was compared to our optimized process (Figure 1 and Supplementary Table S1). As shown in Figure 1, two major types of changes were made to this central process step. The first one was related to the construction of the iodixanol gradient; while the conventional method used four layers of iodixanol at different densities, our new protocol only used three layers since the

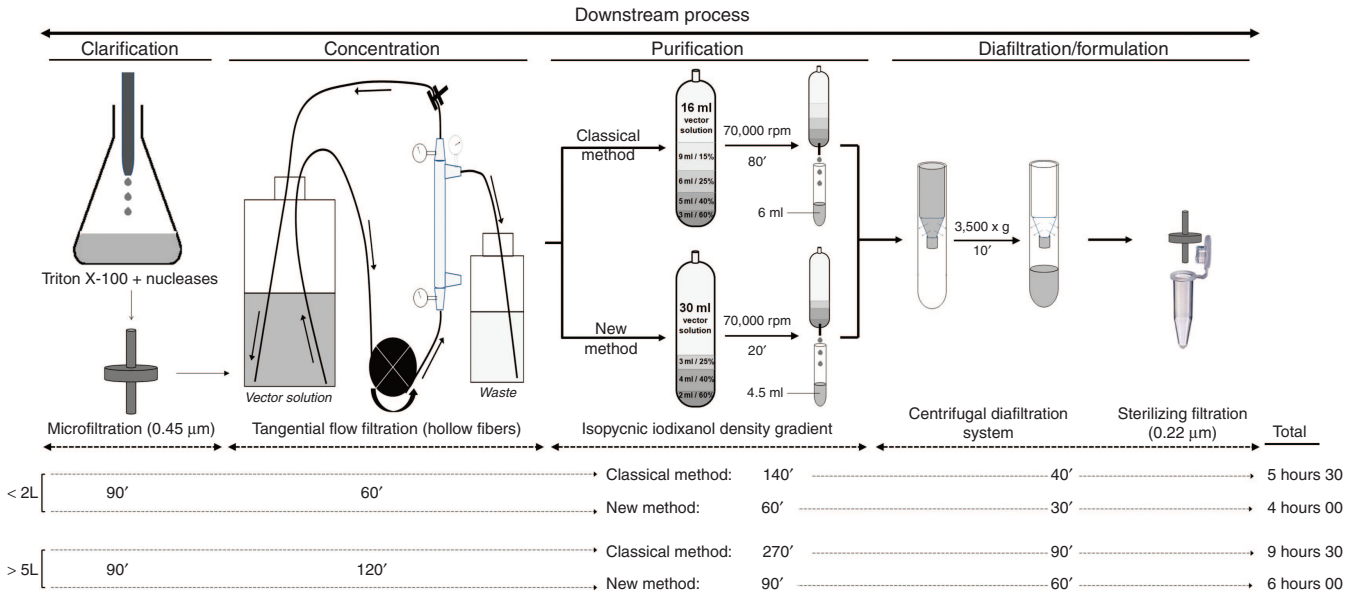

Figure 1 Schematic representation of the downstream process used for the purification of research and pilot-scale recombinant adeno-associated virus (rAAV) vectors produced by baculovirus expression vector system. Research (< 2l) and pilot-scale (> 5l) suspensions were first clarified by addition of Triton X-100 and nucleases before final 0.45 µm dead end microfiltration. Productions performed in Erlenmeyer flasks were centrifuged at high speed (3,500 × g for 30 minutes) before filtration step (see Supplementary Table S1). The clarified lysate was then concentrated by tangential flow filtration to reach about 20× concentration factor. The purification step using ultracentrifugation of concentrated suspension through discontinuous iodixanol gradients was optimized to allow the deposit of larger volumes of vectors per tube (30 ml instead of 15 ml with the conventional method) and to reduce the length of the run by a 4× factor (20 minutes instead of 80 minutes with slightly modified conventional method) and the length of total purification process by 3× factor. The new approach allowed the collection of lower volume of sample after ultracentrifugation, leading to supplemental time reduction of the diafiltration phase. Below the scheme are shown the time scale for each of the downstream process steps. The total time gain between the conventional and novel processes is shown at the bottom right of the figure. Further details on the downstream process are described in material and methods and Supplementary Table S1.

15% density layer was removed. The volumes of each remaining layer were also substantially reduced (3 ml of 25%, 4 ml of 40% and 2 ml of 60% against 6 ml of 25%, 5 ml of 40%, and 3 ml of 60% for the new and classical method, respectively). These modifications allowed the filling of nearly twice the volume of viral suspension (30 ml) per ultracentrifugation tube then that previously described.[25] In addition to reducing the number of tubes by half, these changes also reduced the filling process time (from 10 to 5 minutes per tube for classical and new method respectively). Furthermore, the new purification method allowed the recovery of the viral vectors after 20 minutes of ultracentrifugation (at 70,000 rpm) against 80 minutes using our previous slightly modified conventional method.[26] Following this new protocol, one round of ultracentrifugation instead of two was performed to treat equivalent volumes of production. Moreover, only 4.5 ml of ultracentrifuged product instead of 6 ml was collected, allowing a twofold reduction in the number of diafiltration systems used in the following step. This feature reduced the length of the last purification step as described in Figure 1 and Supplementary Table S1. Finally, unlike the conventional method (lasting 9.5 hours), our optimized method used to treat pilot productions of more than 5 l (> 1×10^{14} viral vectors) allowed to reduce the length of the entire downstream process to a single working day (6 hours).

The new process did not alter productivity, quality, and *in vitro* efficacy of rAAV vectors

The implementation of a new purification method raised the question of its effectiveness in giving equal or even higher vector yields than those obtained using the conventional method. This question was first analyzed through quantitative titration of rAAV. As shown in Figure 2a and Supplementary Table S2, no significant difference in titers was found between the two approaches (7.8×10^{12} and 5.2×10^{12} total vg purified by classical and new method respectively, recovered from three distinct 100 ml productions).

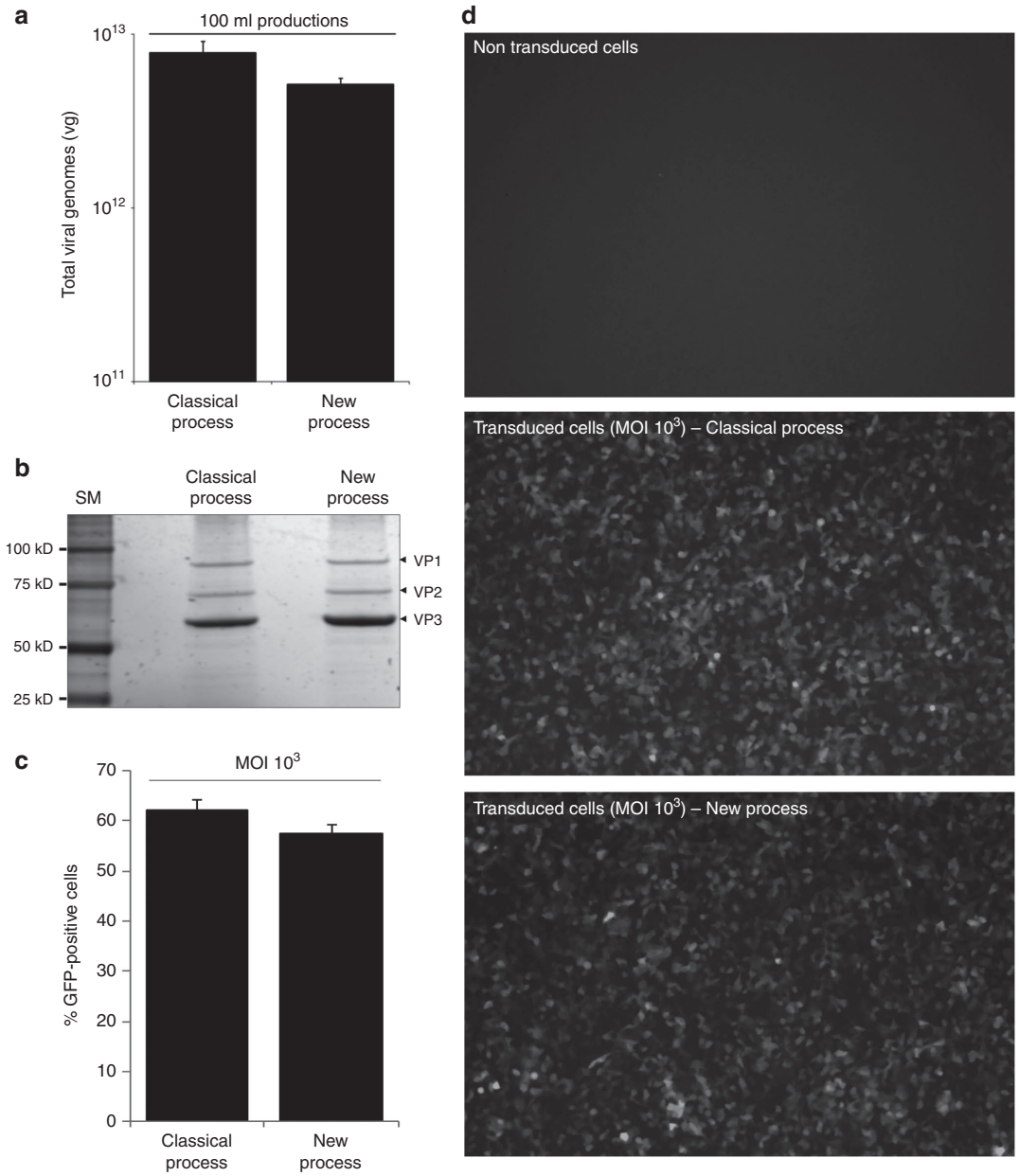

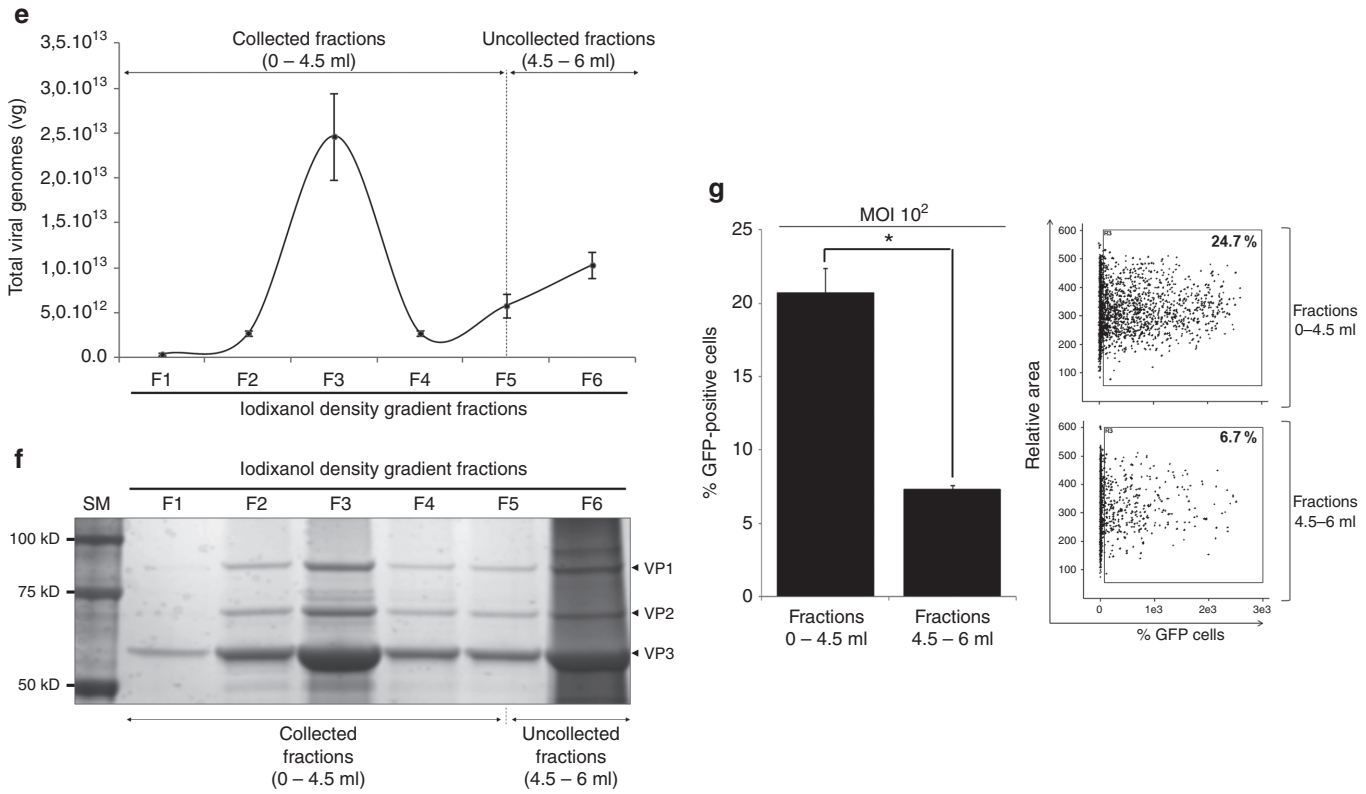

Figure 2 comparative characteristics of recombinant adeno-associated virus (rAAV) purified with classical or new method, and specificities of the new iodixanol density gradient on rAAV particles. (**a**) Quantification by quantitative polymerase chain reaction of the total vg extracted from 100 ml productions purified by conventional or new downstream processes ($n = 3$). No significant difference was observed between the two methods. (**b**) Analysis of the quality of final rAAV products by silver staining of 5.10^{10} vg loaded on SDS-PAGE. The new process lead to same purity levels as the classical method. Capsid proteins VP1, VP2, and VP3 were identified, showing same relative ratio (about 1/1/10 for VP1/VP2/VP3 respectively) for the two processes. (**c**) Flow cytometry quantification of 72 hours post-*in vitro* transduction of HEK293T cells at multiplicity of infection (MOI) of 10^3 showed no significant difference in percentage of GFP-positive cells between vectors recovered from the conventional or the new purification method. (**d**) Fluorescent microscopy of the HEK293T cells 72 hours post-rAAV transduction confirmed the equal efficacy of the two processes to generate functional rAAV without altering cell survival or inducing cell death as observed by homogeneous cell monolayer in both cases (refer also to Supplementary Figure S2 for more results). (**e**) Graphical representation of the quantity of total vg extracted from the first 6 ml fractions collected from suspensions processed with new method ($n = 3$). A peak was observed inside the fraction 3, corresponding to the first milliliter of the 40% iodixanol phase. After a reduction of viral genomes in fraction 4, we observed a slight increase in fractions 5 and 6. The vertical dotted line delineates the collected fractions from the rest of uncollected ultracentrifuged suspension. (**f**) Silver staining of a SDS-PAGE in which identical volumes of each iodixanol fractions were loaded. The relative intensity of the rAAV capsid proteins (VP1, VP2, and VP3) appeared to change similarly to the amount of viral genomes presented in (**e**). Delimitation between collected and uncollected fractions is represented in the bottom of the gel by a vertical dotted line. (**g**) Fluorescence-activated cell sorting (FACS) analysis of GFP-positive HEK293T cells transduced at MOI of 10^2 by rAAV collected from the first 4.5 ml or the next 1.5 ml fraction produced from the new method ($n = 3$). Significant difference in percentage of GFP-positive cells was observed between the two fractions as shown by *($P = 0.03$), indicating the presence of less efficient or defective vectors in the fractions located above the first 4.5 ml. An example of FACS gates is shown in the right part.

Moreover, we analyzed the quality of viral vectors by using 5×10^{10} vg from each purification process by running a sodium dodecyl sulfate polyacrylamide gel electrophoresis (SDS-PAGE) that was thereafter treated for silver staining (Figure 2b). We found no difference in quality between the vectors obtained from the two purification methods. Indeed, in both cases, the level of purity was satisfactory since the conventional viral capsid protein ratio was maintained in both situations (ratio of 1/1/10 for VP1/VP2/VP3 respectively). Of note, on silver-stained SDS-PAGE, we detected a few thin bands which most likely were the result of degraded VPs by baculoviral proteases as previously described.[31,32]

Furthermore, we compared rAAV-GFP vectors through an *in vitro* transduction assay, followed by flow cytometry analysis for a precise quantification of GFP-positive cells. HEK293T cells were transduced with rAAV-GFP recovered from the conventional or new purification methods at different multiplicity of infection. Seventy-two hours post-transduction, cells were visualized by fluorescent microscopy before flow cytometry quantification (Figure 2c,d and Supplementary Figure S2). Independent of the multiplicity of infection used, no significant difference in *in vitro* transduction efficacy was observed between vectors collected from the two methods of purification. Moreover, no cytotoxic effect was observed following microscopy analyses (Figure 2d). We concluded that the new purification process allowed recovering vectors of high quality without any alteration in yields and *in vitro* transduction capacity compared to the rAAV purified by conventional downstream process.

Iodixanol gradient fractionation revealed the distribution of functional and altered rAAV particles

To better characterize the distribution of vector particles inside the new iodixanol gradient set up (Figure 1), we collected milliliter fractions from the bottom of the ultracentrifuged tubes, followed by analysis of the viral genome content by quantitative polymerase chain reaction (Q-PCR). As shown

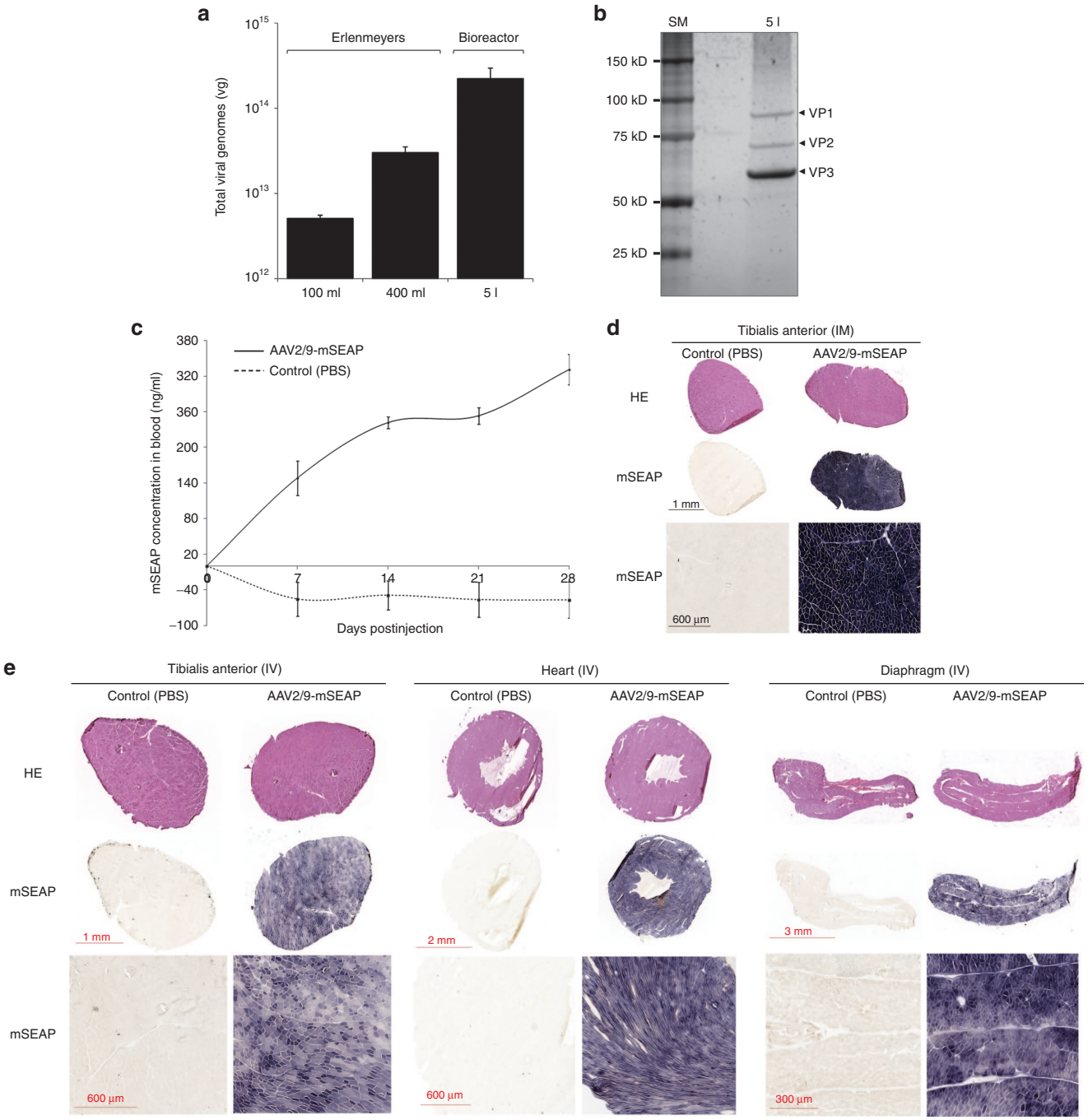

Figure 3 quantitative and qualitative analyses of pilot-scale productions of recombinant adeno-associated virus (rAAV)2/9 vectors processed by the new method, and evaluation of their *in vivo* performances. (**a**) Comparative quantification of total viral genomes extracted from 100 ml, 400 ml and 5l productions ($n = 3$). Linear productivity was observed between the different volumes of productions. Of note, the 100 and 400 ml suspensions were produced in Erlenmeyer flasks whereas the 5l were done in a bioreactor system. Supplementary details on titers and yields are available in Supplementary Table S2. (**b**) The quality of the final rAAV product recovered from 5l production was determined by silver staining of 5×10^{10} vg loaded on SDS-PAGE. The same high-quality vectors than previously described for research-scale productions were obtained (see Figure 2b). The VP ratio was also maintained. (**c**) Analysis of mSEAP concentration in blood of C57BL10 mice intramuscularly injected with rAAV2/9-mSEAP vectors ($n = 3$). Continuous increase in levels of mSEAP was observed within 4 weeks after injection. The lower curve represents the levels of mSEAP in control mice injected with saline solution. (**d**) Histological staining of PBS (left panel) and rAAV2/9-mSEAP (right panel) injected muscle (*Tibialis anterior*). Serial sections were used for hematoxylin-eosin staining (upper sections) and for mSEAP enzymatic staining (middle sections). Microscopic enlargement of the tissue sections is shown in the bottom. Saturating mSEAP expression was observed in rAAV-injected muscles. (**e**) Histological staining of different muscle tissues (TA, heart and diaphragm) originating from C57BL10 mice intravenously (IV) injected with PBS (left panel) or rAAV2/9-mSEAP vectors (right panel). As observed in (**d**), high mSEAP expression was also observed in different tissues, demonstrating the efficacy of rAAV vectors processed with our new purification method to perform whole body treatment. Additional results on IV efficiency of vectors are shown in Figure S3.

in Figure 2e, the graphical distribution of vg gave a Gaussian-like curve with a peak observed in fraction 3 containing collected volumes ranging from 2 to 3 ml. According to the new set up of iodixanol gradient (Figure 1), fraction 3 could correspond to the boundary between the 60 and the 40% phases, confirming the cushion property of the 60% layer, and the role of the 40% layer as an equilibrium phase for the full viral particles.[25] Figure 2e also shows a rise in the level of vg from fraction 5 (volumes ranging from 4 to 5 ml). Since only the first 4.5 ml are collected from our new purification method, we wondered about the nature of these "upper layers viral particles". Of note, we decided to collect the first 4.5 ml rather than the first 6 ml, as carried out with the conventional method, since we observed a significant decrease in the quality of purified products when we collected far from fraction 4 (data not shown). After running 10 µl of each milliliter collected fractions on SDS-PAGE, the gel was subjected to silver staining. As depicted in Figure 2f, the VP band intensities showed a great quantitative correlation with the titration results shown in Figure 2e. Moreover, these results clearly confirmed the deterioration of purity, visually indicated by dark smears, as we collected closer to and mostly after fraction 6. According to the new gradient construction (Figure 1), the upper boundary of fraction 6 should correspond to the limit between the 40 and the 25% layers, explaining the possible new cushion property of this border able to stop many potential contaminants.

Finally, we compared the *in vitro* transduction efficacy of the first 4.5 ml with the following 1.5 ml to determine whether the particles detected by Q-PCR (Figure 2e) and silver staining (Figure 2f) in this last uncollected fraction were still fully functional. A multiplicity of infection of 10^2 was used on HEK293T cells and the percentage of GFP-positive cells was quantified by flow cytometry analysis 72 hours post-transduction (Figure 2g). A significantly higher transduction efficacy was observed when using rAAV particles collected from the first 4.5 ml fraction compared to the following 1.5 ml fraction of the iodixanol gradient ($P = 0.03$). This result showed that the "upper layer particles", as illustrated in Figure 2e, probably contained a large majority of defective interfering particles. The lower density of these defective vectors could suggest the presence of incomplete viral genomes. Of note, it was technically difficult to concentrate fractions beyond the sixth phase due to the high concentration of contaminants causing filter clogging during the buffer exchange procedure. Due to the inability to obtain volumes as concentrated as the previous phases, we did not explore further the content in particles of the upper iodixanol gradient fractions. Nevertheless, we hypothesized that empty rAAV particles might be retained in the 25% phase of the gradient. More extensive subsequent studies will be performed to better characterize the full to empty particle ratio obtained following our process.

The new process was applicable to pilot-scale productions

To determine whether this novel process could be applied to larger scales, we processed up to 400 ml of productions using Erlenmeyer flasks, and 5 l using bioreactor system. The quantification of the total number of viral genomes is shown in Figure 3a and gave a linear rise with 5.1×10^{12}, 3.1×10^{13}, and 2.3×10^{14} total vg purified from three independent processes of 100 ml, 400 ml, and 5 l productions, respectively. Supplementary Table S2 online gives supplementary titration details, showing, for example, a relative constant yield (vg/cell) whatever the volume of production. We also evaluated the quality of the vectors collected from the 5 l process by silver staining of SDS-PAGE (Figure 3b). A high-quality profile was obtained, also respecting the conventional ratio of the natural respective levels of VP1, VP2, and VP3 (1/1/10). Together, these quantitative and qualitative results provided the proof of principle that the optimized process met the requirements for scalable levels of viral vector productions.

In addition, taking into account the previous *in vitro* transduction results between the conventional and the new methodological approaches (Figure 2c,d), we considered that only an *in vivo* transduction assay could truly answer the question of the functionality of rAAV vectors. We focused our investigations on serotype 9 of the AAV, which is well documented for its tropism for muscle tissues.[33–36] We decided to replace the GFP with the mSEAP reporter gene to allow a noninvasive *in vivo* monitoring as previously described.[37] A group of three C57BL/10 adult mice was first intramuscularly injected in *Tibialis anterior* (TA) muscle with 2×10^{12} vg of rAAV2/9-mSEAP vectors. mSEAP protein was weekly monitored in blood for 4 weeks. Figure 3c shows the gradual rise of mSEAP levels in blood over time, compared to phosphate-buffered saline (PBS)-injected mice. One month after vector injection, mice were sacrificed and injected muscles were stained to reveal the levels of mSEAP produced by muscle fibers. Saturating mSEAP signal was observed all over the injected TA (Figure 3d), confirming the great functionality of the rAAV vectors in an *in vivo* environment. To go one step further, we took advantage of high titers obtained from purifications of the 5 l productions to perform whole body treatments by systemic administration of the vectors in order to assess the tissue tropism and global biodistribution of our vectors. Retro-orbital injections of a group of three C57BL/10 adult mice were performed. We collected blood 7 days later and tissues 1 month postinjection (Supplementary Figure S3a). As shown in Supplementary Figure S3b, quantification of the levels of mSEAP in blood 7 days postinjection was compared to the one analyzed in intramuscularly injected mice, and was found to be more than 15-fold higher with 1,600.3 and 108.3 ng of mSEAP per ml of blood between systemic and intramuscular-injected mice respectively. In parallel, different tissue cryosections were stained for mSEAP expression. *TA*, *Triceps brachialis*, hearts, diaphragms, kidneys, and livers were all strongly positive for mSEAP compared to the PBS-injected control mice (Figure 3e and Supplementary Figure S3c), demonstrating the ability of our rAAV2/9 vectors to be largely biodistributed all over the body.

DISCUSSION

Here we show that it is possible, by implementation of simple procedures, to propose a new, rapid, low-cost, and robust rAAV process able to meet the demands of many laboratories in term of quantity and quality of vectors. The use of baculovirus/insect cell system has made a decisive turn toward the industrial mode of production, a required milestone for the use of innovative therapies based on gene transfer to future patients with cancer, genetic, or neurodegenerative diseases. The baculovirus/insect cell system confers ultimately the possibility of scaling up the levels of production much more than can be provided by processes using HEK293T adherent cells. This flexibility in volumes of production is an advantageous characteristic for institutions practicing research and development and interested in advancing their therapeutic projects from the laboratory to the clinic. It is important to notice that the baculovirus expression vector system is no longer the only proposed production system capable of scaling up the levels of production.

Competing upstream process approaches have emerged such as those using derived HEK293 cells able to grow in suspension[14] or the use of stable cell lines or Herpex simplex virus.[15,16] These interesting systems, using transfection protocols, remain nevertheless highly dependent on large quantities and good quality of plasmids required for the production of viral vectors, characteristics particularly important in view of good manufacturing processes grade productions for the delivery of clinical batches. Alternatively, the use of BIIC as raw material necessary to start rAAV production in insect cell cultures appears as another turning point in the quest for baculovirus cryo-conservation, but also for simplification and significant reduced costs of the upstream process.[29] The use of infectious recombinant baculoviruses allows subsequent amplification of vector production that is finally extended to the whole initial insect cell culture 72 hours post-BIIC inoculation. For example, by cryo-preserving 200 ml of BIIC per new recombinant baculovirus, constituting a master cell bank (Supplementary Figure S1), we could theoretically process about 2,000 l of rAAV production. Obviously, the initial volumes of produced BIIC could be amplified well beyond the previous example.

The advantages conferred by the rapid scaling up of production levels necessarily raise the question of the subsequent purification steps. Here, we show that two important phases of the downstream process allow significant improvements in terms of duration and consequently sample volumes able to be processed. The first important point concerns the concentration process by tangential flow filtration (TFF). There is currently a large number of concentrating systems available from different manufacturers. Tangential ultrafiltration hollow fibers or cassettes exhibit a wide range of products differentiated by their cut-off, the nature of the membranes, and the filter surfaces. By rigorously establishing all of these parameters on small-scale productions, as we previously performed, it becomes possible to easily define their equivalents for larger volumes. Moreover, the availability of automated TFF systems, able to control both the transmembrane pressure as well as the levels of concentration factors provide an ergonomic and secure environment to the manipulator, and facilitate even more the speed of the process. These developments now allow us to ensure a relative homogeneity in the TFF duration between small and large volumes for identical concentration factors. Indeed, by defining, for instance, a constant filtrate flux rate of 15 l/m^2/hour, we can easily calculate the required filter surfaces related to the original sample volumes to be treated. Here, we confirm that this process can be performed with a difference of only 1 hour of TFF treatment between our research and pilot-scale productions. Indeed, as described later, 25 l of sample have required less than 3 hours to be 30× concentrated (higher concentration factor than used in this work).

On another hand, the real novelty presented here concerns the important optimization made to the set up and processing of the iodixanol density gradient. The majority of publications describing purification of AAV vectors by discontinuous iodixanol gradients refer to the initial work of Zolotukhin *et al*.[25] As presented in this work, the published gradient set up was originally done by successive deposition of four layers of iodixanol solutions at various concentrations (15, 25, 40, and 60%) over which the vector suspension is deposited. In the original article, the authors have used a first 9 ml phase of 15% iodixanol at 1 M NaCl. Addition of NaCl was justified as necessary to destabilize ionic interactions between macromolecules and AAV particles. This necessity was implemented in the process because the iodixanol gradient was used immediately after cell lysis, followed by low-speed centrifugation to simply remove the resulting large cell debris. In our protocol, clarification step using detergent and nucleases followed by tangential ultrafiltration drastically reduced the macromolecular complexes in the viral suspension before its deposit on iodixanol gradient. Indeed, in these experimental conditions, the viscosity of our concentrated solution was relatively low. The first reason is the consequence of nucleases treatment performed during cell lysis. The other point concerns the use of serum-free medium instead of serum-supplemented media used for productions performed in HEK293T cell cultures. Altogether, these observations led us to deeply change the construction of iodixanol gradients with the objective of both increasing the initial amount of viral suspension that can be processed per run and decreasing the time of ultracentrifugation. Our results show that the classical 15% phase of the iodixanol gradient (at 1M NaCl) is clearly dispensable, allowing its replacement by equivalent volume of vector suspension. The adjustment of the volumes of the other phases to 2 ml, 4 ml and 3 ml instead of 5, 5, and 6 ml for the 60, 40, and 25% phases, respectively allow us to fill 30 ml of concentrated vectors per ultracentrifuge tubes (39 ml maximum volume capacity) instead of 15 ml as specified in the original publication. The twofold increase of the volumes per tube coupled to the upstream TFF concentration factor significantly increased the purification capacity of the iodixanol gradient approach. Moreover, after several empirical assays, we were surprised to observe that no significant difference in titers was found between suspensions ultracentrifuged for 80 or 20 minutes, a fall of titers becoming significant for shorter periods (data not shown). Knowing that a Ti70 rotor type supports up to eight tubes of ultracentrifugation, it is possible to treat up to 240 ml of viral suspension in just 20 minutes. If this volume of viral suspension derived from a usual 30 to 40 times concentrated solution, it then turns out that a single 20 minutes run of ultracentrifugation is able to process a starting raw production of approximately 10 l. Considering the fact that less than 30 minutes are now sufficient to prepare series of 8 density-gradient tubes, it becomes easy to imagine the possibility offered by this new approach to perform nearly a dozen runs per working day and per single manipulator without many technical difficulties. In an industrial context, one can imagine to advantageously implement series of ultracentrifuge systems to easily multiply the level of purification capacity offered by our new iodixanol gradient approach. Therefore, we believe that such a process, considered originally as restricted solely to research scales due to the limitation imposed by the volumes able to be treated by ultracentrifugation, can now be considered for the purification of pilot or even industrial-scale productions. Of note, the following diafiltration step, using in this work centrifugal filtration units as reformulation systems, can easily be replaced by TFF systems to be more compatible with industrial requirements. Finally, the costs generated by our downstream process can be considered negligible compared to competing described processes as previously discussed in the introduction.

These promising process developments obviously pushed us to compare and verify the yields, quality, but also the efficiency of AAV vectors generated by our new technological approach. Our quantitative results show a good linearity between research and pilot-scale productions made in Erlenmeyer flasks and bioreactor respectively. Moreover, the codon optimization of the *rep* and the *cap* genes was an important prerequisite for optimal expression of the resulting proteins in an insect cell environment.[12,28] Our results clearly confirm the well-conserved quality of the viral vectors by using our new purification approach, and no significant difference in the *in vitro* transduction efficacy was observed between vectors recovered

from the conventional and the optimized process. Nevertheless, a subsequent analysis of the full to empty particle ratio will be necessary to complete the quality control of our new AAV process.

In addition, newly processed rAAV vectors produced at scale (5 l) showed high intramuscular efficacy. The results from intravenous administration also demonstrated the capacity of these vectors to spread all over the body through transduction of muscular and nonmuscular tissues. Altogether, these observations confirm once again that the optimized process does not affect the quality and functionality of AAV vectors.

One could point out the fact that in this study we did not exceed volumes of production higher than 5 l. Our first response is that technology of production by bioreactors automated systems is strictly controlled and designed to allow a gradual transition to the large volumes, thus keeping linearity between production levels. The same linearity characteristic is found with the tools and technologies available for the downstream processes. Moreover, as briefly discussed above, we recently processed 25-l productions for treatment of Golden Retriever muscular dystrophic dogs, a canonical animal model of Duchenne muscular dystrophy.[38] The titers obtained by the implementation of our new downstream process exceeded 10^{15} vg, opening the door to whole body treatments on adult dogs for preclinical studies. The technological details and results of this project will be the subject of a future communication. Nevertheless, our results show that this optimized process is compatible with the scaling up of the vector productions towards larger volumes, maintaining high titers, short process duration, and low costs.

MATERIALS AND METHODS

Recombinant baculovirus and BIIC production processes

Codon-optimized *Rep78/52* gene (from AAV2 serotype) was generated as previously described.[28] The codon-optimized Cap9 gene (from AAV9 serotype) was generated as previously described for the Cap2 gene.[12] Briefly, the wild-type Cap9 gene (provided by the Penn Vector Core, University of Pennsylvania, Pennsylvania, USA) was amplified by PCR as described.[12] A schematic representation of the Cap9 nucleotide modifications is shown in Supplementary Figure S4. The resulting $Rep2_{opt}$ and $Cap9_{opt}$ genes were then cloned in pFastBac Dual plasmid following instructions provided with the Bac-to-Bac baculovirus expression system kit (Thermo Fisher Scientific, Illkirch, France). Briefly, the $Rep78/52_{opt}$ and $Cap9_{opt}$ genes were cloned under the control of the pPolh (polyhedrin) and the p10 baculoviral promoters respectively to produce the pFBD-Rep2/$Cap9_{opt}$ donor plasmid. Constructions harboring GFP or mSEAP cDNAs, inserted between the two AAV2 inverted terminal repeats (ITR), and controlled by the Cytomegalovirus (CMV) promoter, were cloned in pFastBac 1 plasmid to produce the pFBD-GFP or pFBD-mSEAP donor plasmids respectively. The pFBD-Rep2/$Cap9_{opt}$, pFBD-GFP, and pFBD-mSEAP were each transformed in DH10Bac competent *Escherichia coli* cells to produce, by transposition mechanism, the pBAC-Rep2/$Cap9_{opt}$, pBAC-GFP, or pBAC-mSEAP recombinant baculoviral genomes respectively. As recommended by the manufacturer, the pBAC genomes were transfected with Cellfectin II transfection reagent (Thermo Fisher Scientific) into Sf9 insect cell line (Thermo Fisher Scientific) to produce rBAC-Rep2/$Cap9_{opt}$, rBAC-GFP or rBAC-mSEAP recombinant baculovirus vectors. Sf9 cells were grown either in adherent or in nonadherent conditions in SFX medium (GE Healthcare, Pasching, Austria) without any serum supplementation. Five rBAC clones of each original construction were picked up from viral plaque assay and amplified through two consecutive infectious passages in Sf9 cells. 24 hours after the last infectious process performed in up to 400 ml of Sf9 cell suspension, baculovirus-infected insect cells (BIIC) were generated[29,30] and 1 to 5 ml aliquots at 10^7 BIIC/ml were immediately cryopreserved in 7.5% dimethylsulfoxide solution diluted in previous conditioned SFX medium.

AAV upstream process

A ratio BIIC versus Sf9 cells of 1 to 10^4 (v/v) was used to initiate the production of AAV vectors. For the upstream process, the insect cells were cultivated in nonadherent conditions in serum-free SFX medium. Research-scale productions (from 20 ml to 2 l) were performed using 125 ml to 3l Erlenmeyer flasks with vented cap (Corning, Amsterdam, The Netherlands) placed in agitator incubators warmed at 26 °C and set to 110 rpm rotary shaking. Pilot-scale productions (5 l) were performed in "wave-type" Biostat Cultibag RM bioreactors (Sartorius AG, Göttingen, Germany) set to 20 rocks per minute, 26 °C, 7% rocking angle and 450 ml per minute of air flow rate injected into the culture bag. Seventy-two hours postinfection, the culture was stopped and prepared for downstream process.

AAV downstream process

The clarification step was initiated by insect cells disruption using 0.5% final concentration of Triton X-100 detergent (in both Erlenmeyer and bioreactor systems). RNAse A (Sigma-Aldrich, Saint-Quentin Fallavier, France) was added at a final concentration of 5 µg/ml and the culture was maintained at 37 °C for 1 hour under shaking. For research-scale productions (20 ml to 2 l), the suspension was first centrifuged at 3,500 × g for 20 minutes before filtration through a 0.45 µm polyethersulfone membrane syringe filter unit of 33 mm diameter (Millipore, France) for productions up to 100 ml, or a 0.8–0.45 µm double layer polyethersulfone membrane filter of 17.3 cm^2 (Sartorius AG) for productions up to 2 l. For 5-l pilot-scale productions, a 20 µm polypropylene prefilter membrane of 500 cm^2 (Sartorius AG) was first used to retain large debris before the use of a 0.8–0.45 µm polyethersulfone filter of 300 cm^2 of filtration surface (Sartorius AG) to finalize the clarification step.

For volumes greater than 400 ml of cultures, a step of concentration by TFF was performed through a polyethersulfone membrane hollow fiber unit with 500 kDa molecular weight cut off placed on an automated Kros Flow Research IIi TFF system (Spectrum Laboratories, Breda, The Netherlands). 115 to 490 cm^2 filtration surfaces were used for 400 ml to 2 l productions respectively, and a 1,550 cm^2 filtration surface was used for the 5 l productions. A 20× concentration factor was reached in both cases, leading to a final volume of 60 and 240 ml respectively (refer to Supplementary Table S1).

The purification step was performed by an isopycnic ultracentrifugation which was slightly modified from the previously described protocol.[25] What we defined as "classical or conventional process" in the text was performed by filling 16 ml of viral suspension through a glass Pasteur pipette in the bottom of 25 × 89 mm Quick-Seal Polyallomer dome-top tube (Beckman Coulter, Villepinte, France). This suspension was raised up by successive addition of 9 ml of 15% iodixanol (from 60% stock solution; Sigma-Aldrich) at 1M NaCl, 6 ml of 25% iodixanol, 5 ml of 40% iodixanol, and 3 ml of 60% iodixanol. Iodixanol solutions were all diluted in 1× PBS-MK buffer (1M NaCl, 1 mmol/l MgCl2, 2.5 mmol/l KCl, 1× PBS). Tubes were heat-sealed with the Tube topper system (Beckman Coulter), placed in Ti70 rotor, and ultracentrifuged at 70,000 rpm for 80 minutes in an Optima L100XP ultracentrifuge (Beckman Coulter). The Fraction Recovery system (Beckman Coulter) was used to puncture the tube from the bottom side and the six first milliliters, containing viral particles, were collected. Our "new process" proposed an optimization of the previous method by adding up to 30 ml of the viral suspension in the centrifuge tubes before addition of 3 ml of 25% iodixanol, 4 ml of 40% iodixanol, and 2 ml of 60% iodixanol. For this new process, 20 minutes of ultracentrifugation was performed to recover the AAV particles in the first 4.5 ml of the tube bottom. Diafiltration was done through centrifugal concentration and filtration unit Amicon Ultra-15 (Millipore, Guyancourt, France) according to the manufacturer instructions. The diafiltration was performed three times leading to a 450 times dilution factor of the original collected solution. A 0.22 µm polyvinylidene difluoride membrane of 0.1 or 0.65 cm^2 (Millipore, Villepinte, France) was used for sterilizing filtration of the diafiltrated solution issue from research-scale or pilot-scale productions respectively.

AAV genome titration by Q-PCR

AAV genomes were titered as previously described.[26] Briefly, 5 µl of purified vector was treated 30 minutes at 37 °C with 5 µl of DNAse I at 2U/µl (Thermo Fisher Scientific). Five microliters of Proteinase K at 20 mg/ml (Thermo Fisher Scientific) were added to previous mixture, followed by 1 hour incubation at 56 °C. Ten microliters of pretreated solution were serially diluted to obtain 10^{-2} to 10^{-7} of AAV genome dilutions. Taqman Q-PCR was performed by using the iTaq Universal Probes Supermix (Bio-Rad, Marnes-la-Coquette, France), 0.1 µmol/l of AAV22mers forward primer (5′-CTCCATCACTAGGGGTTCCTTG-3′), 0.3 µmol/l of AAV12mers reverse primer (5′-GTAGATAAGTAGCATGGC-3′), and 0.1 µmol/l of AAV_MGB.P Fam Taqman probe (5′-TAGTTAATGATTAACCC-3′, Thermo Fisher Scientific). Fifteen microliters of the previous Taqman mix were added to 10 µl of

diluted AAV genome. In parallel, 10 µl of serially diluted AAV plasmid, containing ITR2 sequences (from 10^8 to 10^2 copies per well) was deposited in duplicates to serve as plasmid range. PCR was run in CFX96 Touch Real-Time PCR Detection System (Bio-Rad) under the following conditions: hold at 95 °C for 15 minutes, and 40 cycles at 95 °C/15 seconds, and 54 °C/1 minute. Raw data were exported and analyzed by the BioRad CFX manager software. Titration results were given in viral genomes/ml (vg/ml).

Determination of AAV purity by silver staining of SDS-PAGE

Purity of recombinant AAV vectors was assessed on SDS-PAGE by loading 5×10^{10} vg on 4–12% NuPage Bis-Tris gels (Thermo Fisher Scientific) run under reducing conditions. After migration, proteins and nucleic acid content was revealed by using Silver Staining Plus protocol (Bio-Rad Laboratories) following manufacturer instructions. The gel was deposited on white tray for picture acquisition by Gel Doc EZ system and analyzed by the Image Lab software (Bio-Rad).

In vitro assays and FACS analyses

In vitro assays were performed in 24-well tissue culture plates having 2 cm^2 of growth area per well. 2×10^5 HEK293T cells per well were seeded in total volume of 300 µl of 1× Dulbecco's modified Eagle medium supplemented with Glutamax, 4.5 g/l of D-Glucose (Thermo Fisher Scientific), 10% of fetal bovine serum (Biowest, France), and 1% of Penicillin-Streptomycin solution (Life Technologies). Twenty-four hours later, an average of the number of cells per well was determined by trypsinization and automatic cell counting. Vector transduction was performed with rAAV2/9-GFP at logarithmic multiplicity of infection ranging from 10 to 10^4. Forty-eight hours later, cells were observed by inverted fluorescent microscopy (Leica Microsystems, Nanterre, France) to verify the efficiency of AAV transduction through GFP expression. For quantitative measures, the cell monolayers were first trypsinized and centrifuged at 600 × g for 5 minutes. The pellet was resuspended in 4% paraformaldehyde solution and fixation was done for 10 minutes at room temperature. After centrifugation (600 × g/5 minutes), the fixed cells were homogenized in 1× PBS supplemented with 1% fetal bovine serum. Determination of the percentage of GFP-positive cells was performed by flow cytometry using the ImageStreamX Mark II Amnis Imaging Flow Cytometer (Merk Millipore, Darmstadt, Germany) through the INSPIRE and IDEAS software for acquisition and analysis operations respectively. The cytometry experiments were performed on CYMAGES facility (University of Versailles, Montigny-le-Bretonneux, France).

In vivo assays

All studies on mice were conducted in strict accordance with the institutional guidelines for animal research transposed from the European directive 2010/63/EU. Project authorization, including all the procedures, was submitted to the Ministry of Higher Education and Research on 31 March 2014. All injections were performed after inhalational anesthesia using isoflurane, and all efforts were made to minimize animal number, procedure lengths, and suffering. Ten-week-old C57BL/10 mice (three animals per group) were injected intramuscularly with 50 µl of AAV2/9-mSEAP vectors issued from the new purification process. A total of 2.0×10^{12} vg was injected in TA muscles. Fifty microliters of blood were withdrawn every week for 1 month, and serum was isolated by blood centrifugation at 10,000 × g for 5 minutes at 4 °C. Mice were sacrificed 1 month postinjection by cervical dislocation and TA muscles were harvested. TA muscles were immediately frozen in liquid nitrogen-cooled isopentan solution and cryopreserved at −80 °C.

Ten-week-old C57BL/10 mice (three animals per group) were also injected intravenously through retro-orbital delivery of 1.0×10^{13} vg per gram of body mass. To enhance biodistribution, the vectors were diluted in 1× PBS for a final injection volume of 100 µl per mouse. A unique blood collection (50 µl) was performed at day 7 and mice were sacrificed 1 month postinjection. TA, triceps, heart, diaphragm, kidney, and liver were immediately frozen as previously described and cryopreserved at −80 °C. Serial 10-µm cryosections were made and examined for alkaline phosphatase enzymatic activity. Histological slides were first fixed with 0.5% glutaraldehyde solution for 15 minutes at room temperature followed by three cycles of 15 minutes washing with 1× PBS. To inactivate endogenous alkaline phosphatase activity, slides were incubated at 65 °C for 30 minutes in PBS, followed by two PBS washings. 5-Bromo-4-Chloro-3 Indolyphosphate/Nitro Blue Tetrazolium solution (Sigma-Aldrich) was added to cryosections and incubated at 37 °C for 30 minutes to several hours until occurrence of significant visual colored staining, compared to slides of noninjected muscles. Quantification of mSEAP from mouse serum was performed with the Phospha-Light SEAP Reporter Gene Assay System (Thermo Fisher Scientific) according to manufacturer instructions. Briefly, serum was first 50-fold diluted in a dilution buffer provided with the Phosphalight kit before endogenous alkaline phosphatase inactivation at 65 °C for 30 minutes. After sixfold serial dilutions in assay and reaction buffers containing chemiluminescent substrates and enhancers, microplates were placed in a luminometer for luminescence detection. Raw data were analyzed through simple spreadsheet and quantified using using a standard curve previously prepared by serially diluting stock enzyme.

Statistical analyses

Graphical representations are presented as mean ± standard error of means, and a two-tailed Student's *t*-test is used to determine significant differences in percentage of GFP-positive cells between iodixanol fractions 0–4.5 and 4.5–6 ml (Figure 2g). $P < 0.05$ represented by * in Figure 2g, is considered as significant.

CONFLICT OF INTEREST

The authors declare no conflict of interest.

ACKNOWLEDGMENTS

This work was supported by the Association Monegasque Contre les Myopathies and Duchenne Parent Project France. The authors thank Amalia Stantzou for proofreading and correcting the manuscript.

REFERENCES

1. Balakrishnan, B and Jayandharan, GR (2014). Basic biology of adeno-associated virus (AAV) vectors used in gene therapy. *Curr Gene Ther* **14**: 86–100.
2. Gaudet, D, Méthot, J, Déry, S, Brisson, D, Essiembre, C, Tremblay, G *et al.* (2013). Efficacy and long-term safety of alipogene tiparvovec (AAV1-LPLS447X) gene therapy for lipoprotein lipase deficiency: an open-label trial. *Gene Ther* **20**: 361–369.
3. Salmon, F, Grosios, K and Petry, H (2014). Safety profile of recombinant adeno-associated viral vectors: focus on alipogene tiparvovec (Glybera®). *Expert Rev Clin Pharmacol* **7**: 53–65.
4. Kotterman, MA and Schaffer, DV (2014). Engineering adeno-associated viruses for clinical gene therapy. *Nat Rev Genet* **15**: 445–451.
5. Bainbridge, JW, Smith, AJ, Barker, SS, Robbie, S, Henderson, R, Balaggan, K *et al.* (2008). Effect of gene therapy on visual function in Leber's congenital amaurosis. *N Engl J Med* **358**: 2231–2239.
6. Hauswirth, WW, Aleman, TS, Kaushal, S, Cideciyan, AV, Schwartz, SB, Wang, L *et al.* (2008). Treatment of leber congenital amaurosis due to RPE65 mutations by ocular subretinal injection of adeno-associated virus gene vector: short-term results of a phase I trial. *Hum Gene Ther* **19**: 979–990.
7. Maguire, AM, Simonelli, F, Pierce, EA, Pugh, EN Jr, Mingozzi, F, Bennicelli, J *et al.* (2008). Safety and efficacy of gene transfer for Leber's congenital amaurosis. *N Engl J Med* **358**: 2240–2248.
8. Yue, Y, Ghosh, A, Long, C, Bostick, B, Smith, BF, Kornegay, JN *et al.* (2008). A single intravenous injection of adeno-associated virus serotype-9 leads to whole body skeletal muscle transduction in dogs. *Mol Ther* **16**: 1944–1952.
9. Xiao, X, Li, J and Samulski, RJ (1998). Production of high-titer recombinant adeno-associated virus vectors in the absence of helper adenovirus. *J Virol* **72**: 2224–2232.
10. Grimm, D, Kern, A, Rittner, K and Kleinschmidt, JA (1998). Novel tools for production and purification of recombinant adenoassociated virus vectors. *Hum Gene Ther* **9**: 2745–2760.
11. Salvetti, A, Orève, S, Chadeuf, G, Favre, D, Cherel, Y, Champion-Arnaud, P *et al.* (1998). Factors influencing recombinant adeno-associated virus production. *Hum Gene Ther* **9**: 695–706.
12. Urabe, M, Ding, C and Kotin, RM (2002). Insect cells as a factory to produce adeno-associated virus type 2 vectors. *Hum Gene Ther* **13**: 1935–1943.
13. Mietzsch, M, Grasse, S, Zurawski, C, Weger, S, Bennett, A, Agbandje-McKenna, M *et al.* (2014). OneBac: platform for scalable and high-titer production of adeno-associated virus serotype 1-12 vectors for gene therapy. *Hum Gene Ther* **25**: 212–222.
14. Chahal, PS, Schulze, E, Tran, R, Montes, J and Kamen, AA (2014). Production of adeno-associated virus (AAV) serotypes by transient transfection of HEK293 cell suspension cultures for gene delivery. *J Virol Methods* **196**: 163–173.
15. Martin, J, Frederick, A, Luo, Y, Jackson, R, Joubert, M, Sol, B *et al.* (2013). Generation and characterization of adeno-associated virus producer cell lines for research and preclinical vector production. *Hum Gene Ther Methods* **24**: 253–269.
16. Ye, GJ, Scotti, MM, Thomas, DL, Wang, L, Knop, DR and Chulay, JD (2014). Herpes simplex virus clearance during purification of a recombinant adeno-associated virus serotype 1 vector. *Hum Gene Ther Clin Dev* **25**: 212–217.

17. Okada, T, Nonaka-Sarukawa, M, Uchibori, R, Kinoshita, K, Hayashita-Kinoh, H, Nitahara-Kasahara, Y *et al.* (2009). Scalable purification of adeno-associated virus serotype 1 (AAV1) and AAV8 vectors, using dual ion-exchange adsorptive membranes. *Hum Gene Ther* **20**: 1013–1021.
18. Qu, G, Bahr-Davidson, J, Prado, J, Tai, A, Cataniag, F, McDonnell, J *et al.* (2007). Separation of adeno-associated virus type 2 empty particles from genome containing vectors by anion-exchange column chromatography. *J Virol Methods* **140**: 183–192.
19. Urabe, M, Xin, KQ, Obara, Y, Nakakura, T, Mizukami, H, Kume, A *et al.* (2006). Removal of empty capsids from type 1 adeno-associated virus vector stocks by anion-exchange chromatography potentiates transgene expression. *Mol Ther* **13**: 823–828.
20. Anderson, R, Macdonald, I, Corbett, T, Whiteway, A and Prentice, HG (2000). A method for the preparation of highly purified adeno-associated virus using affinity column chromatography, protease digestion and solvent extraction. *J Virol Methods* **85**: 23–34.
21. Auricchio, A, Hildinger, M, O'Connor, E, Gao, GP and Wilson, JM (2001). Isolation of highly infectious and pure adeno-associated virus type 2 vectors with a single-step gravity-flow column. *Hum Gene Ther* **12**: 71–76.
22. Koerber, JT, Jang, JH, Yu, JH, Kane, RS and Schaffer, DV (2007). Engineering adeno-associated virus for one-step purification via immobilized metal affinity chromatography. *Hum Gene Ther* **18**: 367–378.
23. Lock, M, Alvira, MR and Wilson, JM (2012). Analysis of particle content of recombinant adeno-associated virus serotype 8 vectors by ion-exchange chromatography. *Hum Gene Ther Methods* **23**: 56–64.
24. Hermens, WT, ter Brake, O, Dijkhuizen, PA, Sonnemans, MA, Grimm, D, Kleinschmidt, JA *et al.* (1999). Purification of recombinant adeno-associated virus by iodixanol gradient ultracentrifugation allows rapid and reproducible preparation of vector stocks for gene transfer in the nervous system. *Hum Gene Ther* **10**: 1885–1891.
25. Zolotukhin, S, Byrne, BJ, Mason, E, Zolotukhin, I, Potter, M, Chesnut, K *et al.* (1999). Recombinant adeno-associated virus purification using novel methods improves infectious titer and yield. *Gene Ther* **6**: 973–985.
26. Dias Florencio, G, Precigout, G, Beley, C, Buclez, PO, Garcia, L and Benchaouir, R (2015). Simple downstream process based on detergent treatment improves yield and *in vivo* transduction efficacy of adeno-associated virus vectors. *Mol Ther Methods Clin Dev* **2**: 15024.
27. Lock, M, Alvira, M, Vandenberghe, LH, Samanta, A, Toelen, J, Debyser, Z *et al.* (2010). Rapid, simple, and versatile manufacturing of recombinant adeno-associated viral vectors at scale. *Hum Gene Ther* **21**: 1259–1271.
28. Smith, RH, Levy, JR and Kotin, RM (2009). A simplified baculovirus-AAV expression vector system coupled with one-step affinity purification yields high-titer rAAV stocks from insect cells. *Mol Ther* **17**: 1888–1896.
29. Cecchini, S, Virag, T and Kotin, RM (2011). Reproducible high yields of recombinant adeno-associated virus produced using invertebrate cells in 0.02- to 200-liter cultures. *Hum Gene Ther* **22**: 1021–1030.
30. Wasilko, DJ, Lee, SE, Stutzman-Engwall, KJ, Reitz, BA, Emmons, TL, Mathis, KJ *et al.* (2009). The titerless infected-cells preservation and scale-up (TIPS) method for large-scale production of NO-sensitive human soluble guanylate cyclase (sGC) from insect cells infected with recombinant baculovirus. *Protein Expr Purif* **65**: 122–132.
31. Kaba, SA, Salcedo, AM, Wafula, PO, Vlak, JM and van Oers, MM (2004). Development of a chitinase and v-cathepsin negative bacmid for improved integrity of secreted recombinant proteins. *J Virol Methods* **122**: 113–118.
32. Hitchman, RB, Possee, RD, Crombie, AT, Chambers, A, Ho, K, Siaterli, E *et al.* (2010). Genetic modification of a baculovirus vector for increased expression in insect cells. *Cell Biol Toxicol* **26**: 57–68.
33. Fang, H, Lai, NC, Gao, MH, Miyanohara, A, Roth, DM, Tang, T *et al.* (2012). Comparison of adeno-associated virus serotypes and delivery methods for cardiac gene transfer. *Hum Gene Ther Methods* **23**: 234–241.
34. Katwal, AB, Konkalmatt, PR, Piras, BA, Hazarika, S, Li, SS, John Lye, R *et al.* (2013). Adeno-associated virus serotype 9 efficiently targets ischemic skeletal muscle following systemic delivery. *Gene Ther* **20**: 930–938.
35. Kornegay, JN, Li, J, Bogan, JR, Bogan, DJ, Chen, C, Zheng, H *et al.* (2010). Widespread muscle expression of an AAV9 human mini-dystrophin vector after intravenous injection in neonatal dystrophin-deficient dogs. *Mol Ther* **18**: 1501–1508.
36. Schinkel, S, Bauer, R, Bekeredjian, R, Stucka, R, Rutschow, D, Lochmüller, H *et al.* (2012). Long-term preservation of cardiac structure and function after adeno-associated virus serotype 9-mediated microdystrophin gene transfer in mdx mice. *Hum Gene Ther* **23**: 566–575.
37. Bartoli, M, Poupiot, J, Goyenvalle, A, Perez, N, Garcia, L, Danos, O *et al.* (2006). Noninvasive monitoring of therapeutic gene transfer in animal models of muscular dystrophies. *Gene Ther* **13**: 20–28.
38. Vulin, A, Barthélémy, I, Goyenvalle, A, Thibaud, JL, Beley, C, Griffith, G *et al.* (2012). Muscle function recovery in golden retriever muscular dystrophy after AAV1-U7 exon skipping. *Mol Ther* **20**: 2120–2133.

Supplementary Information accompanies this paper on the *Molecular Therapy—Methods & Clinical Development* website (http://www.nature.com/mtm)